ISSN 1674-1056
http://cpb.iphy.ac.cn
http://iopscience.iop.org/cpb
中国物理 B
Chinese Physics
中国物理
Chinese Physics B

Wettabilities of Si and Al-12Si alloy on Pd-implanted 6H-SiC

Ting-Ting Wang(汪婷婷), Gui-Wu Liu(刘桂武), Zhi-Kun Huang(黄志坤), Xiang-Zhao Zhang(张相召), Zi-Wei Xu(徐紫巍), Guan-Jun Qiao(乔冠军)
Citation: Chin. Phys. B . 2018, 27(4): 046101. **doi:** 10.1088/1674-1056/27/4/046101

Journal homepage: http://cpb.iphy.ac.cn; http://iopscience.iop.org/cpb

What follows is a list of articles you may be interested in

Quantitative determination of anti-structured defects applied to alloys of a wide chemical range

Jing Zhang(张静), Zheng Chen(陈铮), Yongxin Wang(王永欣), Yanli Lu(卢艳丽)
Chin. Phys. B . 2016, 25(11): 116102. **doi:** 10.1088/1674-1056/25/11/116102

Comparative study on beryllium and magnesium as a co-doping element for ZnO:N

Yu-Quan Su(苏宇泉), Ming-Ming Chen(陈明明), Long-Xing Su(苏龙兴), Yuan Zhu(祝渊), Zi-Kang Tang(汤子康)
Chin. Phys. B . 2016, 25(6): 066106. **doi:** 10.1088/1674-1056/25/6/066106

Theoretical analysis of the influence of flexoelectric effect on the defect site in nematic inversion walls

Gui-Li Zheng(郑桂丽), Hui Zhang(张辉), Wen-Jiang Ye(叶文江),Zhi-Dong Zhang(张志东), Hong-Wei Song(宋宏伟), Li Xuan(宣丽)
Chin. Phys. B . 2016, 25(3): 036101. **doi:** 10.1088/1674-1056/25/3/036101

Krypton ion irradiation-induced amorphization and nano-crystal formation in pyrochlore $Lu_2Ti_2O_7$ at room temperature

Xie Qiu-Rong, Zhang Jian, Yin Dong-Min, Guo Qi-Xun, Li Ning
Chin. Phys. B . 2015, 24(12): 126103. **doi:** 10.1088/1674-1056/24/12/126103

Influences of neutral oxygen vacancies and E_1'centers on α-quartz

Li Hui-Ran, Cheng Xin-Lu, Zhang Hong, Zhao Feng
Chin. Phys. B . 2015, 24(10): 106105. **doi:** 10.1088/1674-1056/24/10/106105

Wettability of Si and Al–12Si alloy on Pd-implanted 6H–SiC*

Ting-Ting Wang(汪婷婷)[1], Gui-Wu Liu(刘桂武)[1,†], Zhi-Kun Huang(黄志坤)[1], Xiang-Zhao Zhang(张相召)[1], Zi-Wei Xu(徐紫巍)[1], and Guan-Jun Qiao(乔冠军)[1,2,‡]

[1] *School of Materials Science and Engineering, Jiangsu University, Zhenjiang* 212013, *China*
[2] *State Key Laboratory for Mechanical Behavior of Materials, Xi'an Jiaotong University, Xi'an* 710049, *China*

(Received 4 December 2017; revised manuscript received 22 January 2018; published online 10 March 2018)

SiC monocrystal substrates are implanted by Pd ions with different ion-beam energies and fluences, and the effects of Pd ion implantation on wettability of Si/SiC and Al–12Si/SiC systems are investigated by the sessile drop technique. The decreases of contact angles of the two systems are disclosed after the ion implantation, which can be attributed to the increase of surface energy (σ_{SV}) of SiC substrate derived from high concentration of defects induced by the ion-implantation and to the decrease of solid–liquid surface energy (σ_{SL}) resulting from the increasing interfacial interactions. This study can provide guidance in improving the wettability of metals on SiC and the electronic packaging process of SiC substrate.

Keywords: ceramics, defects, surfaces, ion implantation, wettability

PACS: 61.72.U–, 68.08.Bc, 65.40.gp, 68.55.Ln **DOI:** 10.1088/1674-1056/27/4/046101

1. Introduction

Silicon carbide (SiC), as a promising wide band-gap material, has been widely used in high power, high frequency, and high temperature semiconductor devices. The fabrication of a SiC semiconductor device involves ion implantation and heterogeneous interfacial bonding closely related to wettability. Actually, the wettability of SiC by molten metals plays a critical role in the brazing of SiC ceramic components, the preparing of metal–SiC composite, and the electronic packaging of SiC substrate.[1,2] However, the wettability of the metal/SiC system is not always so good as required. According to Young's equation: $\cos\theta = (\sigma_{SV} - \sigma_{SL})/\sigma_{LV}$ (where σ_{ij} denotes the characteristic surface energies of the solid (S)–liquid (L)–vapor (V) system), there are two main technological approaches to improving the wettability: 1) increasing σ_{SV} and/or simultaneously reducing the σ_{SL} by modifying the ceramic surface; 2) reducing the σ_{SL} by adding interfacial active elements to the metal for enhancing the interfacial interactions between the metal and the substrate.

Presently, there are a few investigations focused on surface modification of SiC to improve the wettability of the metal/SiC system by liquid phase sintering,[2] plasma pulses,[3] and electroless plating[4,5] techniques. Compared with these techniques, ion implantation can possess many advantages such as non-thermal, non-equilibrium process and no interface, change both the surface crystal structure and phase composition,[6,7] and fabricate PiN diodes.[8] Therefore, ion implantation into the ceramic substrate can cause the wettability of the metal/SiC system to change. For instance, our group obtained a significant improvement in the wettability of Ni(–56Si) on the SiC monocrystal substrate by Mo ion implantation, and found that the contact angle was almost completely picked up after succeeding high-temperature annealing treatment on the Mo-implanted SiC substrate.[9] However, Barlak *et al.* concluded that the Ti-implantation on sintered SiC ceramic cannot improve the wettability of Cu on the SiC substrate in their experiments.[10] In particular, our recent investigation showed that Pd ion implantation reduced the wettability of the Al/SiC reactive system.[11]

In this paper, SiC monocrystal substrates are implanted with Pd ions at room temperature, and the effects of Pd ion implantation on wettability of Si/SiC and Al–12 (all in unit wt%) Si/SiC systems are investigated and analyzed based on the variations of substrate surface characteristics and interfacial microstructures. The Pd is selected as an implantation element due to its relatively high melting point and low reactivity with SiC substrate. Our results show that the Pd ion implantation can improve the wettability of the non- and low reactive (Si/SiC and Al–12Si/SiC) systems to different degrees, and this study can further demonstrate the role of ion implantation in determining the wettability of the metal/SiC system.

2. Experiment

The commercially available double-side polished n-type 6H–SiC (0001) monocrystal substrates were implanted with two fluences of Pd ions (5×10^{16} ions/cm^2, 5×10^{17} ions/cm^2) at two acceleration voltages (20 keV, 40 keV) and room temperature. The lattice damages or disorders and the electrova-

*Project supported by the National Natural Science Foundation of China (Grant Nos. 51572112 and 51172177), the Natural Science Foundation of Jiangsu Province, China (Grant No. BK20151340), the Six Talent Peaks Project of Jiangsu Province, China (Grant Nos. 2014-XCL-002 and TD-XCL-004), the Innovation/Entrepreneurship Program of Jiangsu Province, China (Grant No. [2015]26), and the Qing Lan Project of Jiangsu Province, China (Grant No. [2016]15).

†Corresponding author. E-mail: gwliu76@ujs.edu.cn
‡Corresponding author. E-mail: gjqiao@ujs.edu.cn

© 2018 Chinese Physical Society and IOP Publishing Ltd

lences of surface elements of the Pd-implanted SiC substrates were characterized by Rutherford backscattering spectrometry in channeling geometry (RBS/C), Raman spectroscopy, and x-ray photoelectron spectroscopy (XPS). The displacement per atom (dpa) and Pd ion distribution on the Pd-implanted SiC substrate were simulated by the Monte Carlo software SRIM2008. The wetting behaviors of Si and Al–12Si alloy on the as-received SiC and Pd-implanted SiC substrates were evaluated by a high temperature contact angle measuring instrument (OCA15LHT-SV, Dataphysics). The two kinds of wetting samples were heated to 1430 °C and 1050 °C at a heating rate of 5 °C/min in a vacuum of $\sim 4 \times 10^{-4}$ Pa, respectively. After the wetting tests, some couples of samples were selected and immersed in saturated NaOH distilled-water solution to dissolve the solidified drops in order to expose the interface beneath the drop after they had been mechanically removed from the most part. The interfacial microstructures were observed and analyzed by a scanning electron microscope (SEM) coupled with an energy dispersive spectroscope (EDS).

3. Results and discussion

Monte Carlo simulation has been widely used in ion implantation experiments for simulating the dpa distribution and ion concentration profile. Figure 1 shows the variations of dpa and Pd concentrations with depth on the Pd-implanted SiC surfaces generated by different implantation doses and voltages. The maximum implantation damages are essentially centered at depths of $\sim$ 8, 8, and 12 nm with the dpa levels of 193, 1930, and 2190 for implanting Pd ion concentraions of 20 keV/5×10^{16} ions/cm^2, 20 keV/5×10^{17} ions/cm^2, and 40 keV/5×10^{17} ions/cm^2, respectively. It reveals that a high level of lattice damages can be produced by the Pd ion implantation, and that a positive proportional relationship can be clearly seen between the damage level and the implantation energy or fluence. The largest concentrations of Pd ions are located at centers of 15, 15, and 21 nm corresponding to 20 keV/5×10^{16} ions/cm^2, 20 keV/5×10^{17} ions/cm^2, and 40 keV/5×10^{17} ions/cm^2, respectively, indicating that the implantation energy directly affects the depth of Pd ion.

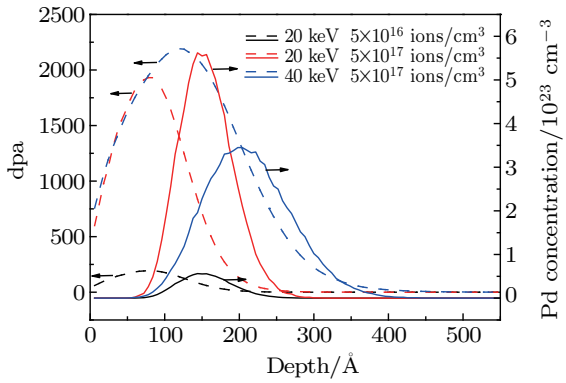


Fig. 1. (color online) Variations of dpa and Pd concentrations with depth, obtained from SRIM simulation.

The RBS/C technique is powerful for determining the disorder accumulation of the ion-implanted sample. Figure 2(a) shows the aligned and random RBS/C spectra of the as-received and Pd-implanted (40 keV/5×10^{17} ions/cm^2) SiC substrates. The aligned spectrum of Pd-implanted SiC (black line) shows the higher aligned yields than the as-received one (green line, no peak), suggesting that the lattice disorder is induced by the Pd ion implantation. The ratio of aligned-to-random yield of the Pd-implanted sample is about 2:3, indicating a high level of lattice disorder on the surface. The presence of Pd in the implanted SiC substrate is verified by the peak centered at 423 keV. The increase in the Si random yield indicates the accumulation of defects (vacancies and interstitials). The random peak of Si shifts from $\sim$ 295 keV to 260 keV, indicating the formation of Si vacancies after the Pd ion implantation.[12] The result provides evidence that the dpa centered at $\sim$ 12 nm can be mainly related to vacancies. A similar trend should be observed for C, but the corresponding signal is overwhelmed by the background signal and therefore is hard to analyze.[12]

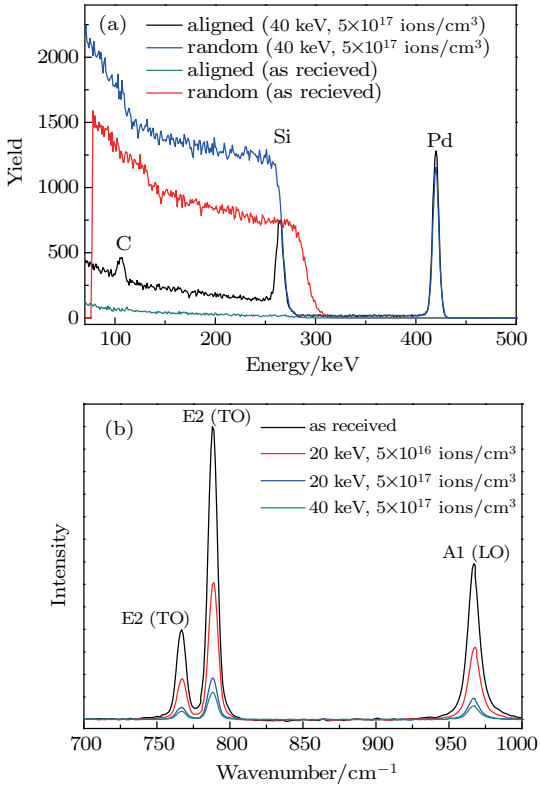


Fig. 2. (color online) (a) RBS/C aligned and random spectra, and (b) Raman spectra of the as-received and Pd-implanted SiC substrates, showing the high concentration of surface defects (lattice damage or disorder and vacancies).

The crystalline damage of 6H–SiC substrate, induced by ion implantation under different implantation conditions, is measured by using Raman spectroscopy in a range from 700 cm^{-1} to 1000 cm^{-1}. The results are shown in Fig. 2(b). The three first-order peaks of Si-C vibration at 766, 788, and 966 cm^1 are detected on the as-received single crystal, corresponding to two transverse phonons E2 (TO) and one longitudinal optical phonon A1 (LO) mode, respectively.[13] After the

Pd ion implanation, the three peak positions are still kept there, and the peak intensity gradually decreases with implanted dose and energy increasing. The results indicate that the Pd ion implantation brings about the damage to the crystallinity of SiC single crystal to different degrees since the variation of Raman spectrum is related to the accumulation of defects and to the changes in atomic forces and displacements owing to the breakdown of Si–C bonds.[14]

Figure 3 presents the XPS spectra of the as-received and Pd-implanted (40 keV/5×10^{17} ions/cm^2) SiC substrates. The two survey spectra confirm the presence of Pd after the Pd ion implantation (Fig. 3(a)). As shown in Fig. 3(b), the Pd 3d peaks at 336.9 eV ($3d_{5/2}$) and 342.5 eV ($3d_{3/2}$) can be assigned to PdO,[15] and the peaks at 335.0 eV ($3d_{5/2}$) and 340.5 eV ($3d_{3/2}$) can be assigned to metallic Pd,[16] indicating that the implanted Pd exists mainly as an elementary substance. The O_{1s} peak at 532.8 eV can be derived from Si–O (Fig. 3(c)),[17] and after the Pd ion implantation the O_{1s} core level spectra at 532.8 eV and 530.5 eV are respectively assigned to Si–O and Pd–O (Fig. 3(d)),[18] which is in good agreement with the Pd spectra.

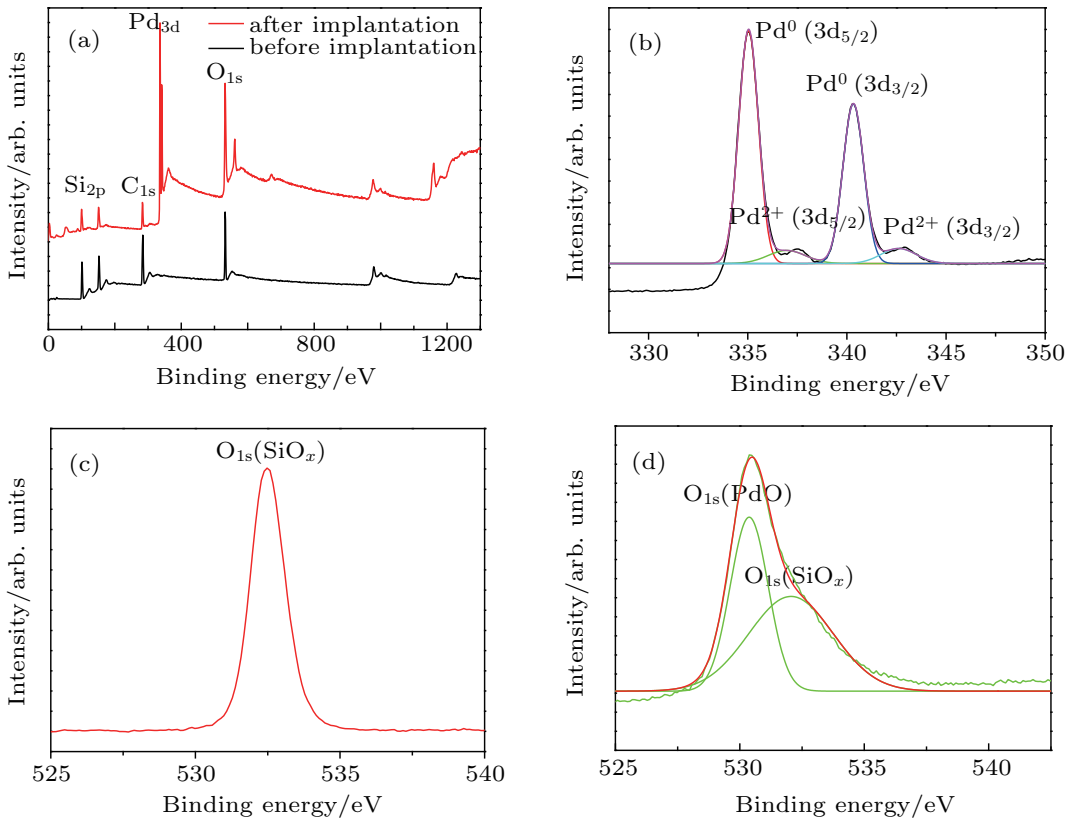


Fig. 3. (color online) XPS spectra of the as-received and Pd-implanted SiC substrates: (a) survey spectra, (b) Pd spectrum, [(c) and (d)] O spectra before and after the Pd ion implantation.

Figure 4(a) presents the variations of contact angle with time for molten Si on the as-received and Pd-implanted SiC substrates at 1430 °C. The equilibrium contact angle of molten Si on the as-received SiC is $\sim 38°$, and it respectively decreases to $\sim 35°$ and 32° while implanting Pd ions of 5×10^{16} ions/cm^2 and 5×10^{17} ions/cm^2, indicating the improvement of wettability of the Si/SiC system after the Pd ion implantation. As mentioned above, a high concentration of defects (lattice damage or disorder and vacancies) induced by the Pd ion implantation can result in the increase of surface energy (σ_{SV}) of SiC substrate. In the wetting experiments, the σ_{LV} of liquid Si remains unchanged at a certain temperature. Moreover, comparing with the non-reactive Si/SiC system, the solid-liquid interfacial energy σ_{SL} can decrease to a certain extent due to the presence of interfacial reactions between the Si drop and Pd at the SiC surface deduced from the Pd–Si phase diagram.[19] As a result, the equilibrium contact angle of Si/SiC system declines more or less according to Young's equation.

Figure 4(b) shows the variations of contact angle with time for molten Al–12Si alloy on the as-received and Pd-implanted SiC substrates at 1050 °C. The equilibrium contact angle of molten Al–12Si alloy on the as-received SiC is $\sim 40°$, and it falls sharply to $\sim 20°$ when implanting the two fluences of Pd ions in spite of the difference in spreading. Moreover, the wetting hysteresis[20] of the Al–12Si/SiC system is weakened and lagged due to the hindering effect of Pd on the formation of dense oxidation film on the SiC substrate surface.

Compared with the Si/SiC system, the Al–12Si/SiC system has an equilibrium contact angle decreasing to a greater extent (Fig. 4), which can be related to the interfacial reactivity after the Pd ion implanation.

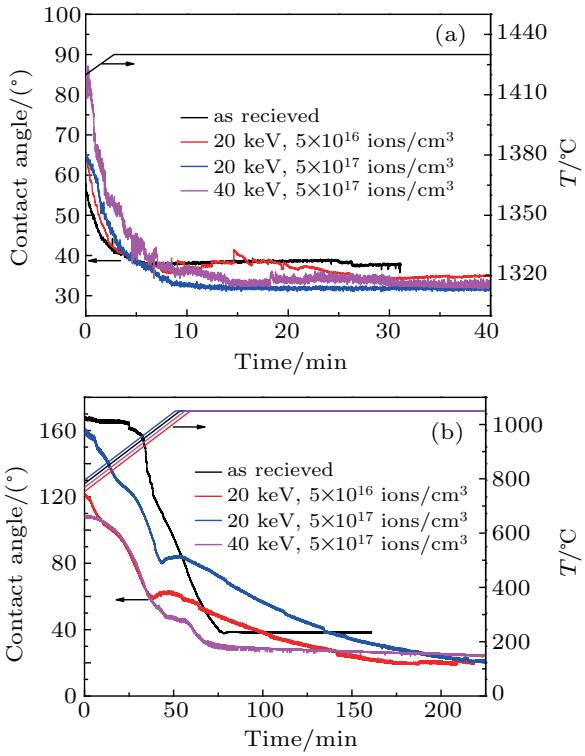


Fig. 4. (color online) Time-dependent contact angles of molten (a) Si and (b) Al–12wt.%Si alloy on the as-received and Pd-implanted SiC substrates, showing the improvement of wettability after the Pd ion implantation.

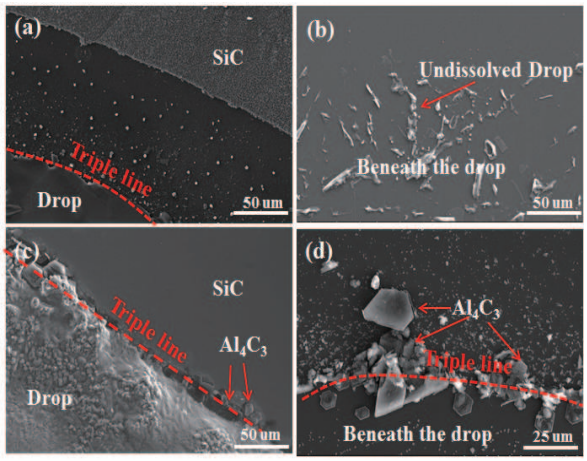


Fig. 5. (color online) Interfacial microstructures of Al–12Si/SiC systems in triple line region and beneath drop [(a) and (b)] before and [(c) and (d)] after the Pd ion implantation of 5×10^{17} ions/cm^2.

Figure 5 shows the interfacial microstructures at the triple line region and beneath the drop of the Al–12Si/SiC system before and after the Pd ion implantation of 5×10^{17} ions/cm^2 respectively. Before the Pd ion implanation, no obvious interfacial reactions can be observed (Figs. 5(a) and 5(b)), which is in good agreement with Lee's prediction, i.e., the interfacial reactivity is quite low when the Si content of Al–Si alloy is close to an equilibrium Si content of $\sim 13.5\%$.[21] However, after the Pd ion implanation platelet-shaped Al_4C_3 crystals are observed (Figs. 5(c) and 5(d)), which can be attributed to the formation of free C atoms on the substrate surface and the direct chemical reaction between Al and C. So, the interfacial interactions are enhanced markedly due to the presence of Pd on the substrate surface, and thus the solid-liquid interfacial energy (σ_{SL}) decreases greatly. Similarly, the surface energy (σ_{SV}) of SiC substrate increases after Pd ion implanation and the σ_{LV} of molten Al–12Si keeps invariant. As a result, the significant decrease of contact angle is obtained according to Young's equation.

4. Conclusions

In this work, two different energies and fluences of Pd ions are implanted into 6H–SiC substrates, and the variations of substrate surface characteristics and of contact angles of Si/SiC and Al–12Si/SiC systems are comparatively investigated before and after ion implantation. The RBS/C and Raman analyses combined with SRIM simulation indicate the high concentration of defects (lattice damage or disorder and vacancies) induced by ion implantation. The presence of Pd, confirmed by XPS analysis, reduces the σ_{SL} to different degrees by enhancing the interfacial interactions between Si or Al–12Si drop and SiC substrate. The equilibrium contact angle of the Si/SiC system declines respectively from 38° to $\sim 35°$ and 32° when concentrations of implanting Pd ions are 5×10^{16} ions/cm^2 and 5×10^{17} ions/cm^2, and the equilibrium contact angle of the Al–12Si/SiC system decreases from 40° to $\sim 20°$. The decrease of contact angle can be reasonably attributed to the decrease of σ_{SL} derived from the enhanced interfacial interactions and to the increase of σ_{SV} of the SiC substrate.

References

[1] Liu G W, Muolo M L, Valenza F and Passerone A 2010 *Ceram. Int.* **36** 1177
[2] Zhao S T, Zhang X Z, Liu G W, Valenza F, Muolo M L, Qiao G J and Passerone A 2015 *Ceram. Int.* **41** 13493
[3] Barlak M, Piekoszewski J and Werner Z 2009 *Surf. Coat. Technol.* **203** 2536
[4] Tekmen C, Saday F, Cocen U and Ljungberg L Y 2008 *J. Compos. Mater.* **42** 1671
[5] Leon C A and Drew R A 2002 *Composites Part A* **33** 1429
[6] Conrad J R, Radtke J L, Dodd R A, Worzala F J and Tran N C 1987 *J. Appl. Phys.* **62** 4591
[7] Qin X F, Liang Y, Wang F X, Li S, Fu G and Ji Y J 2011 *Acta Phys. Sin.* **60** 066101 (in Chinese)
[8] Bu Y, Yoshimoto H, Watanabe N and Shima A 2017 *J. Appl. Phys.* **122** 244504
[9] Zhao S T, Valenza F, Liu G W, Muolo M L, Qiao G J and Passerone A 2014 *Ceram. Int.* **40** 7227
[10] Barlak M, Piekoszewski J, Stanislawski J, Borkowska K, Sartowska B, Werner Z, Miskiewicz M, Jagielski J and Starosta W 2007 *Vacuum* **81** 1271

[11] Huang Z K, Zhang X Z, Wang T T, Liu GW, Shao H C, Wang Y G and Qiao G J 2018 *Surf. Coat. Technol.* **335** 198

[12] Bouziane K, Azri M A, Elzain M, Chérif S M, Mamor M, Declemy A and Thomef L 2015 *J. Alloys Compd.* **632** 760

[13] Nakashima S and Harima H 1997 *Phys. Status Solidi A* **162** 39

[14] Sorieul S, Costantini J M, Gosmain L, Thome L and Grob J J 2006 *J. Phys.: Condens. Matter* **18** 5235

[15] Zhang J T, Suo X Y, Liu X, Liu B K, Xue Y F, Mu L La and Shi H Z 2016 *Mater. Lett.* **184** 25

[16] Zhang Q W, Li J, Liu X X and Zhu Q M 2000 *Appl. Catal. A-Gen.* **197** 221

[17] Cros A, Saoudi R, Hewett C A, Lau S S and Hollinger G 1990 *J. Appl. Phys.* **67** 1826

[18] Militello M C and Simko S J 1994 *Surf. Sci. Spectra* **3** 395

[19] Du Z M, Guo C P, Yang X J and Liu T 2006 *Intermetallics* **14** 560

[20] Cong X S, Shen P, Wang Y and Jiang Q C 2014 *Appl. Surf. Sci.* **317** 140

[21] Lee J C, Park S B, Seok H K, Oh C S and Lee H I 1998 *Acta Mater.* **46** 2635